



Synthesis of highly selective fluorescent peptide probes for metal ions: Tuning selective metal monitoring with secondary structure

Bishnu Prasad Joshi, Keun-Hyeung Lee *

Bio-organic Chemistry Laboratory, Department of Chemistry, Inha University, 253 Younghyun-Dong, Nam-Gu, Incheon-City 402-751, Republic of Korea

ARTICLE INFO

Article history:

Received 28 May 2008

Revised 5 August 2008

Accepted 6 August 2008

Available online 12 August 2008

Keywords:

Peptide

Probe

Selectivity

Metal ions

Turn structure

Sensor

Fluorescence

ABSTRACT

Metal selective fluorescent peptide probes (dansyl-Cys-X-Gly-His-X-Gly-Glu-NH₂, X = Pro or Gly) were developed by synthesizing peptides containing His, Cys, and Glu residues with Pro-Gly sequence to stabilize a turn structure and Gly-Gly sequence to adopt a random coil. The probe containing two Gly-Gly sequences exhibited marked selectivity only for Cu²⁺ over 13 metal ions including competitive transition and Group I and II metal ions under physiological buffer condition. In contrast, the probe containing double Pro-Gly sequences showed high selectivity for Zn²⁺. The peptide probe containing one Pro-Gly sequence exhibited selectivity for Zn²⁺ and Cu²⁺. CD spectra indicated that the secondary structure of the probes played an important role in the selective metal monitoring and a pre-organized secondary structure is not required for the selective detection of Cu²⁺ ion, but is required for the detection of Zn²⁺. We investigated and characterized the binding affinity, binding stoichiometry, reversibility, and pH sensitivity of the peptide probes.

© 2008 Elsevier Ltd. All rights reserved.

1. Introduction

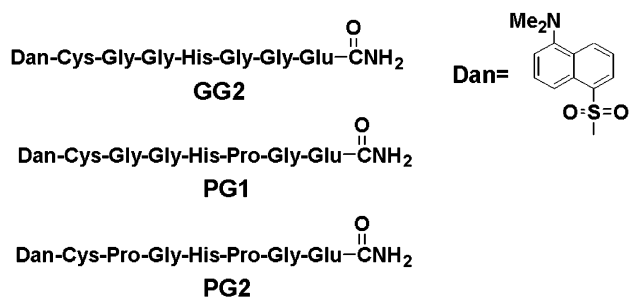
Transition and heavy metal ions play an important role in many biological and environmental processes.^{1,2} Much research effort has focused upon developing various fluorescent probes for the detection of metal ions. Development of metal monitoring peptide probes has received attention for the following reasons³: (1) Peptide probes can be facilely synthesized by solid-phase synthesis; (2) the selectivity and sensitivity for specific metal ions can be optimized by further amino acid replacement⁴; (3) peptide probes can be used in physiological buffer solution due to their high solubility; and (4) peptide probes can be easily conjugated to solid support for further applications.⁵

Several fluorescence peptide probes for monitoring various metal ions were developed.⁴ Most of these consisted of a metal-binding site (receptor) and a signal transduction site (fluorophore).⁴ Binding of the receptor with metal ions resulted in a fluorescent spectrum change of fluorophore as a result of electron or energy transfer.⁶ Much effort in the field of metallo-protein research has resulted in the identification of several small peptide motifs (<15 amino acids) that bind specifically to metal ions.⁷ Several peptide sensors for metal ions have been synthesized on the basis of the primary structures of various metal-binding motifs.⁸ Generally, short peptides containing a metal-binding motif tend to adopt a

random coil structure due to the loss of the protein environments for stabilizing the secondary structure of the binding motif. Thus, the binding affinity and selectivity of short peptide probes are much lower than those of the proteins. It is generally accepted that the pre-organized structures of the short peptide probes are necessary for metal binding. Thus, specific amino acid sequences that stabilize specific secondary structures were included in the primary structures of the probes to improve their metal-binding affinity and selectivity.^{4b,8d,9} However, almost all short peptide probes suffered limitations with binding affinity or selectivity.

In the present study, we investigated whether or not the selective monitoring of a peptide probe for metal ions was tuned by modulating the secondary structure. We designed heptapeptide probes consisting of fluorophore and a metal-binding site due to the easy synthesis and the convenience of the secondary structure characterization by using circular dichroism. 1,5-Dimethylaminonaphthalene sulfonamide (dansyl) group as a fluorophore was introduced to the N-terminal of the peptides because the dansyl group can display a large Stoke shift along with varying quantum yield by changing its local environment.^{6a,8b,10} His, Glu, and Cys residues were frequently found in several metal-binding motifs in various metallo-proteins.^{7,10,11} Previously, we developed a metal-binding peptide probe containing these amino acids.¹² As shown in Scheme 1, we synthesized peptide probes containing these amino acids to afford ligands for metal ions. To change the secondary structure of the peptide probes, a Pro-Gly sequence to stabilize a type II β -turn structure¹³ and a Gly-Gly sequence to

* Corresponding author. Tel.: +82 32 860 7674; fax: +82 32 867 5604.
E-mail address: leekh@inha.ac.kr (K.-H. Lee).



Scheme 1. Chemical structures of peptide probes.

adopt a random coil structure were included in the peptides. We synthesized three peptide probes (**GG2**, dansyl-Cys-Gly-Gly-His-Gly-Gly-Gly-NH₂; **PG2**, dansyl-Cys-Pro-Gly-His-Pro-Gly-Gly-NH₂; **PG1**, dansyl-Cys-Gly-Gly-His-Pro-Gly-Gly-NH₂) by solid-phase peptide synthesis. Notably, **GG2** exhibited great selectivity only for Cu²⁺ among 13 metal ions, including competitive transition metal ions, while **PG2** containing two Pro-Gly sequences showed great selectivity for Zn²⁺. **PG1** containing one Pro-Gly sequence exhibited selectivity for Cu²⁺ and Zn²⁺. We investigated the binding stoichiometry, binding affinity, reversibility, and pH sensitivity of each peptide probe. CD spectra indicated that the secondary structures caused by the Pro-Gly and Gly-Gly sequences changed the selectivity for detecting metal ions. Despite several reports of peptide probes for selective monitoring metal ions, it appears that the first example of the peptide probes' metal selectivity being tuned by modulating the secondary structure.

2. Results and discussion

2.1. Synthesis of peptide probes and their secondary structures

Peptide probes were synthesized by solid-phase peptide synthesis.¹⁴ After cleavage of the crude product from resin, the peptides were purified using semi-preparative HPLC with a C18 column. The successful synthesis and purity (>95%) were confirmed by analytical HPLC with a C18 column and a MALDI TOF mass spectrometer.

To investigate the secondary structures of the peptide probes, the CD spectra of the peptide probes in Hepes buffer solution (pH 7.4) were measured without any co-solvent. CD spectra (Fig. 1) showed that three peptides in the absence of metal ions might adopt different secondary structures. The strong negative bands at 203 nm and near 215 nm indicated that **GG2** containing two Gly-Gly sequences could adopt random coil and β sheet structures, whereas the negative band at 227 nm indicated that **PG1** containing one Pro-Gly sequence might have a turn structure.^{15,16} A negative band at 205 nm and a strong positive band at 225 nm in the CD spectrum of **PG2** were characteristic bands of β hairpin structure.¹⁶ However, CD spectrum with a maximum at 228 nm and a minimum at 205 nm was hallmarks of the polyproline II structure,¹⁷ and the maximum in CD spectrum of a polyproline II could shift to higher or lower wavelengths because of contributions from other secondary structures at nearby wavelengths. Thus, **PG2** containing two Pro-Gly sequences might have a turn structure or a polyproline II structure.

2.2. Fluorescence spectra of probes in the presence of various metal ions

As the peptide probes are fully water soluble, we measured the fluorescence spectrum of the probes in 10 mM Hepes buffer solu-

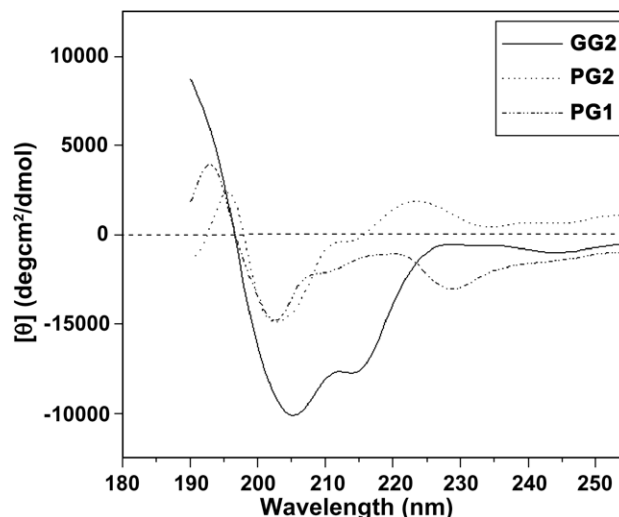


Figure 1. Far UV CD spectrum of peptide probes in 10 mM Hepes buffer solution (pH 7.4).

tion (pH 7.4) without any co-solvent. Fluorescence spectra ranging from 350 to 650 nm were measured by excitation at a wavelength of 330 nm. To investigate metal selectivity of the probes, we measured the fluorescence change of the peptide probes in the presence of various metal cations (Ca²⁺, Cd²⁺, Co²⁺, Pb²⁺, Cu²⁺, Ag⁺, Mg²⁺, Mn²⁺, Ni²⁺, and Zn²⁺ as perchlorate anion; and Na⁺, Al³⁺, and K⁺, as chloride anion). Figure 2 shows the fluorescent emission spectrum of **GG2**, **PG1**, and **PG2** (10 μ M) in Hepes buffer solution (10 mM, pH 7.4) containing each metal ion (1 equiv). **GG2** did not exhibit a fluorescence response with any of the metal ions except Cu²⁺. Upon addition of Cu²⁺, the emission intensity at 510 nm vanished. **PG1** did not have fluorescence response with all test metal ions except Zn²⁺ and Cu²⁺; the emission intensity increased in the presence of Zn²⁺, whereas fluorescence intensity vanished in the presence of Cu²⁺. Figure 2C shows that **PG2** did not exhibit a fluorescence response with almost any of the metal ions including Cu²⁺, except with Zn²⁺ and Cd²⁺. Upon Zn²⁺ addition, the emission intensity of **PG2** at 510 nm increased. Even though Cu²⁺ and Zn²⁺ have similar size and electronic configuration, the peptide probe exhibited great selectivity for Zn²⁺ over Cu²⁺. The fluorescence response of the probes for Zn²⁺ and Cu²⁺ was reversible because the addition of excess EDTA (1–10 equiv) to the probe-metal complex instantly returns in the original metal free emission spectrum [data not shown]. The dansyl fluorophore of these short peptide probes is assumed to directly participate in metal binding. The peptide probes respond with Zn²⁺ by enhancement of emission intensity via a chelation enhanced fluorescence mechanism. However, the probes monitored Cu²⁺ by a fluorescence quenching mechanism utilizing energy or electron transfer of Cu²⁺. Generally, the chemical or peptide sensors containing dansyl moiety and His (imidazole) residue were reported to show a fluorescence response with Cu²⁺ due to the high affinity of the imidazole moiety for Cu²⁺.^{4b,8b,10b} However, **PG2** even containing dansyl and imidazole moiety did not show a fluorescence response with Cu²⁺. In the absence of metal ions, **GG2** showed higher emission intensity than did **PG1**. **PG2** showed the lowest emission intensity at the same concentration. This may be due to the different environment for dansyl group caused by different secondary structures of the peptide probes. Furthermore, we investigated the fluorescence response of the peptide probes to various metal cations in the presence of 140 mM NaCl. The peptide probes showed the same response as measured in Hepes buffer solution without 140 mM NaCl [data not shown].

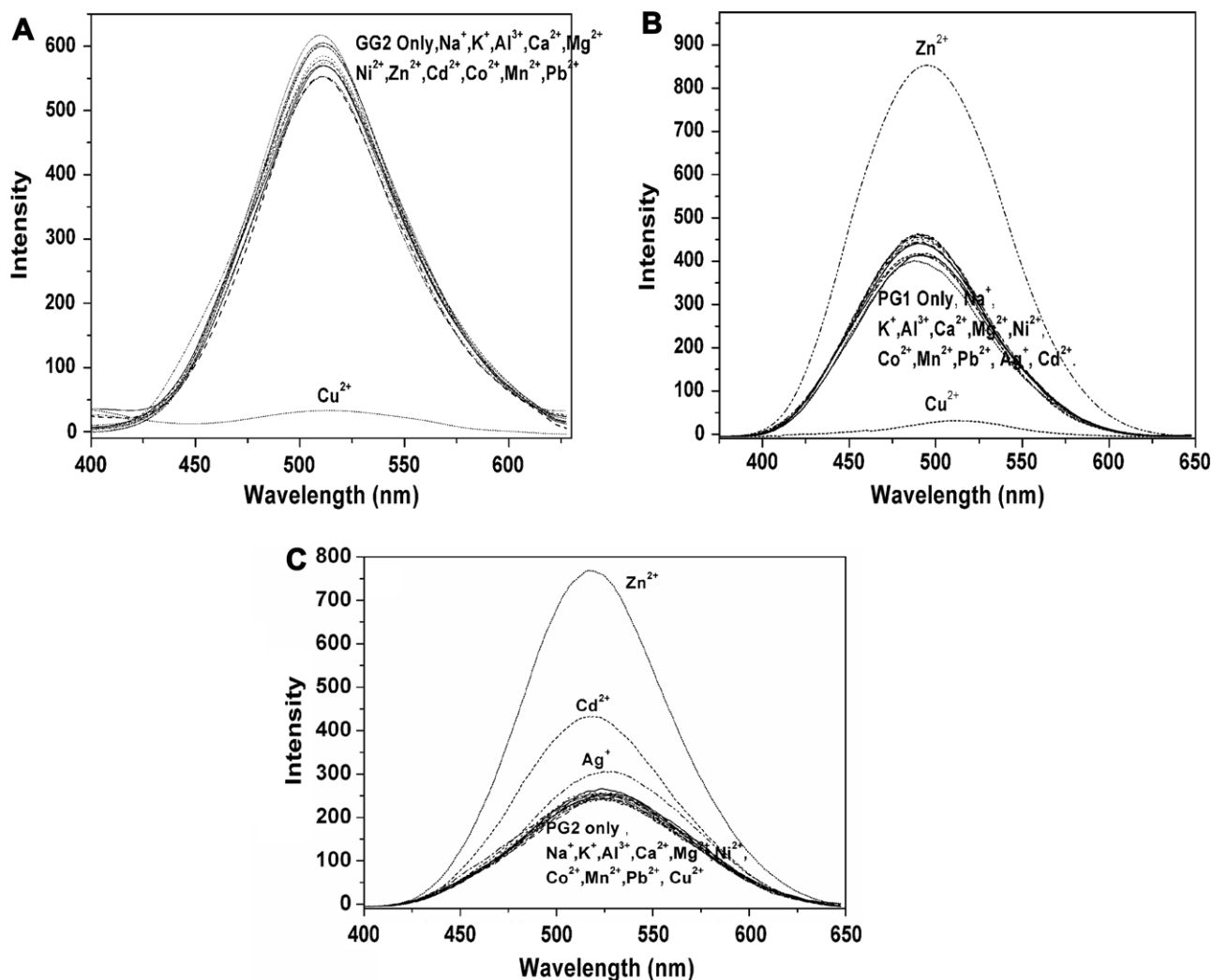


Figure 2. Fluorescence response of (A) **GG2** (10 μM), (B) **PG1** (10 μM), and (C) **PG2** (10 μM) in the presence of various metal ions (1 equiv) in 10 mM Hepes buffer solution (pH 7.4) (excited at 330 nm, excitation slit size 2.5, and emission slit 4.5 nm).

2.3. Binding affinity study

We investigated the binding stoichiometry and affinities of the peptides for Zn^{2+} and/or Cu^{2+} because both metal ions play a vital role in biological functions, such as gene expression, apoptosis, enzyme regulation, and amyloid fibril formation.¹

We used the following criteria to determine binding stoichiometry: Job's plot analysis and the fitting model used for the association constant calculation.¹⁸ To explain the analysis result of each method, data for **PG2** and **GG2** are shown as a representative of all peptide probes. Job's plot analysis was conducted to determine the binding stoichiometry. Job's plot analysis of **PG2** and **GG2** exhibited a maximum at 0.5 mole fraction with Zn^{2+} and Cu^{2+} , respectively (Fig. 3). As suggested by Job's plot, it is likely that **PG2** forms a 1:1 complex with Zn^{2+} in micromolar range and **GG2** also forms a 1:1 complex with Cu^{2+} . However, the Job's plot that was not symmetrical indicated that a more complex equilibrium might be possible, and that the peptides did not form exclusively a 1:1 complex. Imperiali et al. reported that the fluorescent peptide probes forming 1:1 and 1:2 complex exhibited a large shift in the maximum emission wavelength, whereas the peptide forming only a 1:1 complex did not show a shift.^{4b} As shown in Figures 4 and 5, the peptide probe (**GG2**) showed a large shift in the maximum emission intensity when the probes interacted with Cu^{2+} ,

whereas the probe (**PG2**) showed a slight shift in the maximum emission wavelength when the probes interacted with Zn^{2+} .

When we calculated the association constants for Zn^{2+} and Cu^{2+} , we assumed that the peptide probes form a 1:1 complex or a 1:2 complex, respectively. When the probes interacted with Zn^{2+} , the 1:1 complexation model provides a better fit and lower error in the titration (Fig. 4). However, when the probes interacted with Cu^{2+} , the 1:2 complexation model provides a better fitting and lower error in the titration data (Fig. 5). We conclude that even though the peptide probes might have a mixed complex, when the probes interacted with Zn^{2+} , the 1:1 complex might be predominant, whereas, when the probes interacted with Cu^{2+} , the 1:2 complex might be predominant. Table 1 shows the association constants of the peptide probes for Zn^{2+} and Cu^{2+} .

It was expected that inter-disulfide bond formation of the peptide probes in the presence of metal ions would occur because the probes contained a Cys residue. Thus, the peptide probes (10 μM) were incubated in the presence of Zn^{2+} (1 equiv) or Cu^{2+} (1 equiv), respectively. The peptide-metal complex was analyzed by HPLC. HPLC and ESI mass spectrum indicated that disulfide bridged dimer of the peptide probes was not observed [data not shown]. We also measured the binding affinities of the probes for Zn^{2+} and Cu^{2+} in the presence of DTT (1 equiv) as a reducing reagent. This concentration of DTT has no interference effect on the interaction

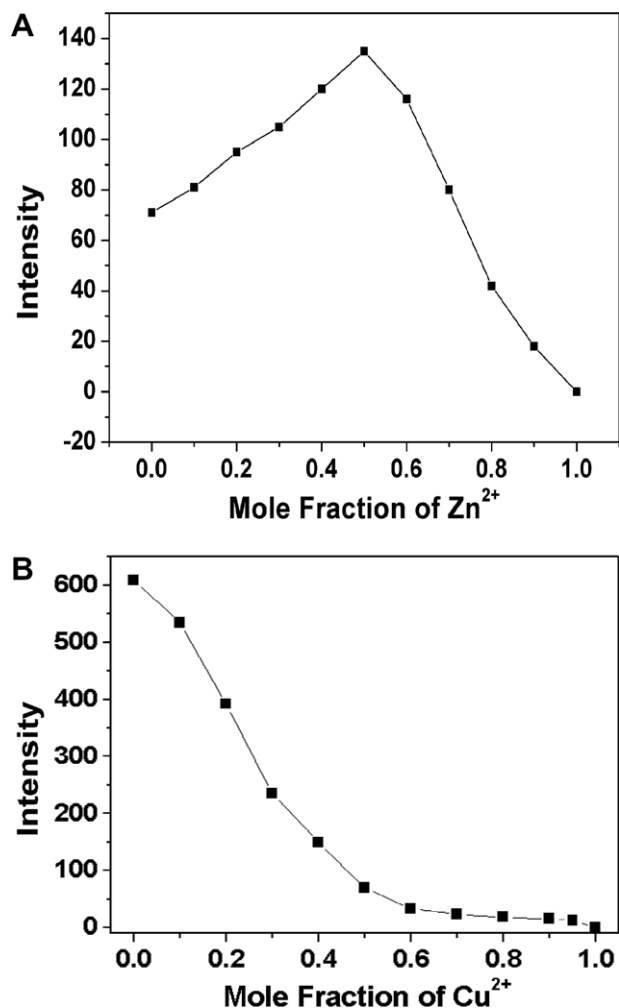


Figure 3. Job's plot for (A) **PG2** and (B) **GG2**. The total [**PG2**] + [**Zn**²⁺] = 2.5 μ M and the total [**GG2**] + [**Cu**²⁺] = 10 μ M.

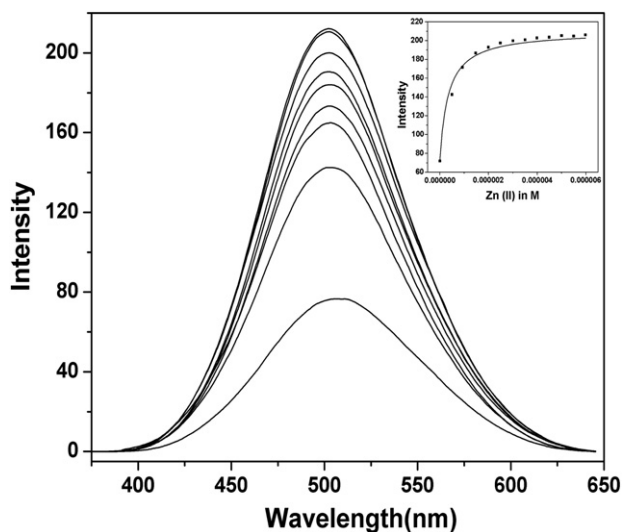


Figure 4. Fluorescence emission spectra of **PG2** upon addition of **Zn**²⁺. Fluorescence emission spectra of **PG2** (2.5 μ M) upon addition of **Zn**²⁺ (0, 0.5, 1.0, 1.5, 2.0, 2.5, 3.0, 3.5, and 4.0 μ M) were measured in 10 mM Hepes buffer (pH 7.4). The fit was obtained from titration data using 1:1 complexation model.

between peptide probes containing two Cys residues with metal ions, and it prevents a disulfide bond formation.¹⁹ The binding

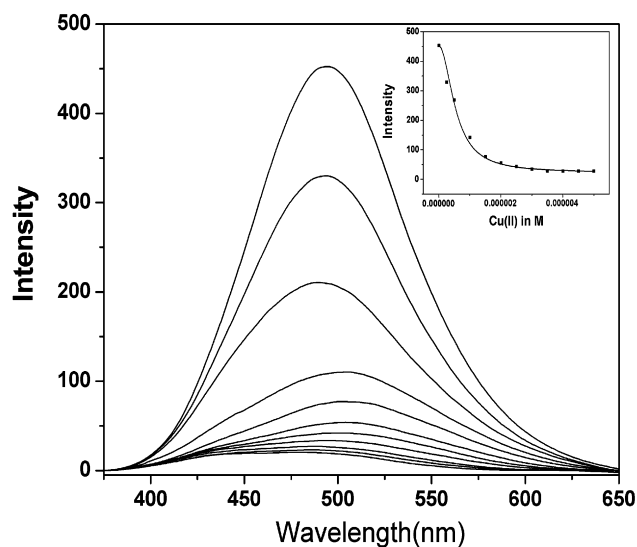


Figure 5. Fluorescence emission spectra of **GG2** upon addition of **Cu**²⁺. Fluorescence emission spectra of **GG2** (2.5 μ M) upon addition of **Cu**²⁺ (0, 0.25, 0.5, 1.0, 1.5, 2.0, 2.5, 3.0, 3.5, 4.0 and 4.5 μ M) were measured in 10 mM Hepes buffer (pH 7.4). The fit was obtained from titration data using 1:2 complexation model.

Table 1

The sequences and association constants of the peptide probes for metal ions at pH 7.4 (10 mM Hepes buffer solution)

Name	Sequence	K_a value for Zn ²⁺ (M^{-1}) 1:1 complex	K_a value for Cu ²⁺ (M^{-2}) 1:2 complex
PG2	Dan-CPGHPGE-NH ₂	$3.0 \pm 0.2 \times 10^6$	NR
PG1	Dan-CGGHPGE-NH ₂	$2.1 \pm 0.1 \times 10^6$	$3.0 \pm 0.4 \times 10^{12}$
GG2	Dan-CGGHGGE-NH ₂	NR	$3.3 \pm 0.4 \times 10^{12}$

NR indicated no response.

affinities of all probes for **Zn**²⁺ and **Cu**²⁺ were not changed in the presence of DTT [data not shown]. The result indicated that the disulfide bond formation of the peptide probes might not occur in the metal-monitoring process.

2.4. Fluorescence spectra change of probes in various pH

We investigated the pH influence on the fluorescence intensity of the peptide probes in the absence and presence of **Cu**²⁺ or **Zn**²⁺. As shown in Figure 6, all peptide probes in the presence or absence of the metal ions exhibited little fluorescence intensity at pH lower than 5.5. This might be due to the protonation of the dimethylamino group ($pK_a \sim 4$) of the dansyl fluorophore.²⁰ At pH > 6.5, the intensity of **GG2** increased by increasing the pH, whereas **GG2-Cu**²⁺ complex exhibited little emission intensity in this pH range (3.5–10.5). The emission intensity difference between **PG1** and **PG1-Zn**²⁺ complex was maintained at pH > 6.5, because the intensity of **PG1** and **PG1-Zn**²⁺ complex similarly increased by increasing pH. However, **PG1-Cu**²⁺ complex exhibited little emission in the whole pH range (3.5–11.5), and the emission intensity difference between **PG1** and **PG1-Cu**²⁺ complex increased with increasing pH. The emission intensity difference between **PG2** and **PG2-Zn**²⁺ complex was the greatest at pH 9.5; the emission intensity of **PG2-Zn**²⁺ complex increased more than 4.5 times than that of **PG2** at this pH. Overall results indicated that the peptide probes are useful for monitoring **Zn**²⁺ or **Cu**²⁺ in the neutral and basic pH.

To investigate the binding affinity change of the probes at a different pH, the association constants of the peptide probes for **Zn**²⁺ and **Cu**²⁺ were measured at pH 11.5 (Table 2). The association con-

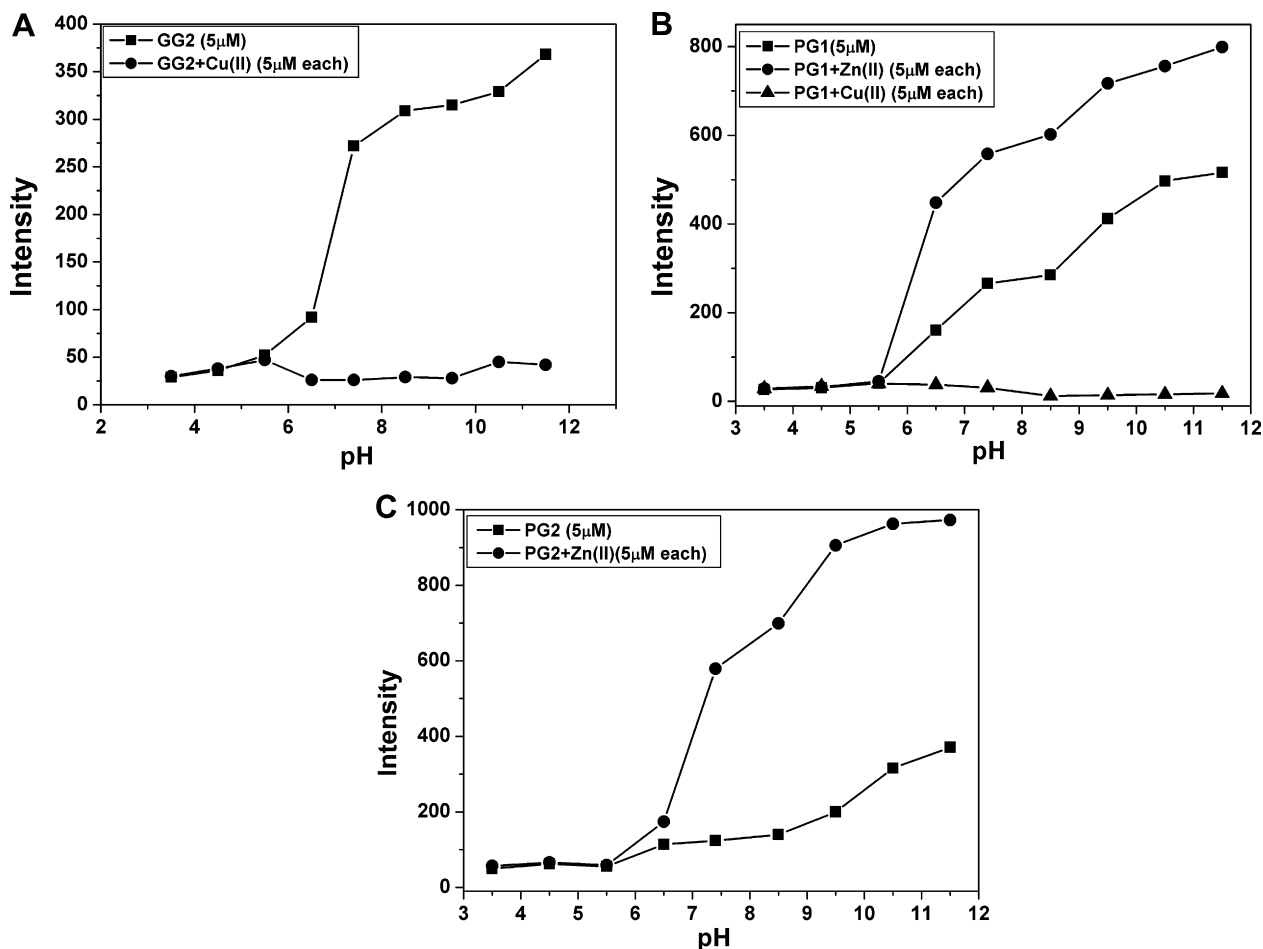


Figure 6. Fluorescence response of (A) **GG2**, (B) **PG1**, and (C) **PG2** in the presence and absence of metal ions (1 equiv) at different pH values.

Table 2

The sequences and association constants of the peptide probes for metal ions at pH 11.5 (10 mM CHES buffer solution)

Name	Sequence	K_a value for Zn^{2+} (M^{-1}) 1:1 complex	K_a value for Cu^{2+} (M^{-2}) 1:2 complex
PG2	Dan-CPGHPGE-NH ₂	$6.8 \pm 0.7 \times 10^6$	NR
PG1	Dan-CGGHPGE-NH ₂	$4.2 \pm 0.5 \times 10^6$	$2.2 \pm 0.2 \times 10^{12}$
GG2	Dan-CGGHGGE-NH ₂	NR	$4.9 \pm 0.1 \times 10^{12}$

NR indicated no response.

stants measured at pH 7.4 and 11.5, indicated that the binding affinities of **PG1** and **PG2** for Zn^{2+} increased with increasing pH, whereas the association constants of **PG1** and **GG2** for Cu^{2+} did not significantly change at higher pH. Considering the pK_a values of Cys, a Cys residue in **PG1** and **PG2** played an important role in the increase of binding affinity for Zn^{2+} at higher pH. To confirm the role of a Cys residue, Cys-protected analogs with acm (acetamidomethyl) groups (**GG2-acm**, dansyl-Cys(Acm)-Gly-Gly-His-Gly-Gly-Glu-NH₂; **PG2-acm**, dansyl-Cys(Acm)-Pro-Gly-His-Pro-Gly-Gly-Glu-NH₂; **PG1-acm**, dansyl-Cys(Acm)-Gly-Gly-His-Pro-Gly-Gly-Glu-NH₂) were synthesized, and fluorescence response was measured at pH 7.4. All Cys-protected analogs did not show any response with Zn^{2+} but with Cu^{2+} . The binding affinities of **GG2-acm** ($K_a = 1.6 \times 10^{12} M^{-2}$) and **PG1-acm** ($K_a = 2.4 \times 10^{12} M^{-2}$) for Cu^{2+} were not significantly different from those of **GG2** and **PG1** for Cu^{2+} . The results indicate that the Cys residue of **PG1** and **PG2** is essential for zinc ion binding, whereas the Cys residue of **GG2**

and **PG1** may not play an important role in Cu^{2+} binding. Generally, the heavy metal-binding motif contained a Cys residue and several potent peptide probes for Zn^{2+} contained Cys residues. This is because the soft ligands, such as the thiol group, are preferred in the binding of Zn^{2+} .^{4b,7a-c,12,19}

2.5. Competition fluorescence study

The concentration of group I and II metal ions in mammalian cells was in the mM range, whereas the transition metal ions in the cell or environment were relatively low. We investigated the fluorescence response of the **GG2**- Cu^{2+} , **PG1**- Zn^{2+} , and **PG2**- Zn^{2+} complexes in the presence of one equivalent of transition metal ions or one hundred equivalent of group I and II metal ions. As shown in Figure 7, the addition of any other metal ion did not change the emission intensity of the **GG2**- Cu^{2+} complex. The zinc-dependent emission intensity of the **PG1**- Zn^{2+} complex was not affected by the presence of any other metal ion except Cu^{2+} (Fig. 8). The binding affinity in Table 1 indicated that **PG1** showed more potent-binding affinity for Cu^{2+} than Zn^{2+} . Even though Cu^{2+} was reported to cause significant quenching for fluorescent chemical and peptide sensors with imidazole and dansyl moiety,^{4b,8b,10b} it is notable that the zinc-dependent fluorescence of **PG2** was not affected by the presence of any other metal ions such as competitive transition metal ions including Cu^{2+} (Fig. 9). **PG2** showed a slight fluorescence response to Cd^{2+} . When the concentration of **PG2** was 2.5 μM , the association constant for Cd^{2+} ($K_a = 1.5 \times 10^6 M^{-1}$) indicated that **PG2** ($K_a = 3.0 \times 10^6 M^{-1}$ with Zn^{2+}) had a

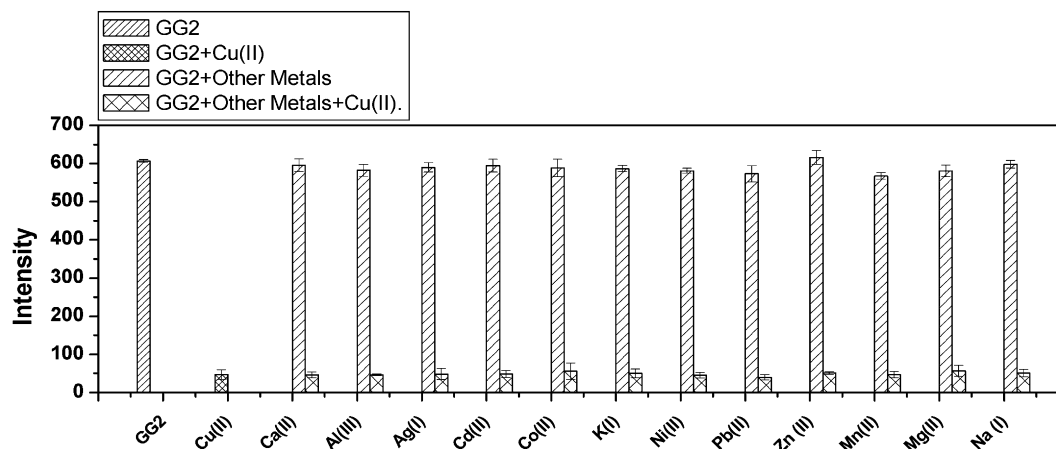


Figure 7. Emission intensity of **GG2** (10 μ M) in the presence of Cu^{2+} (1 equiv) and additional various metal ions at pH 7.4 (10 mM Hepes buffer). All metal ions are evaluated at one equivalent to Cu^{2+} except Na^+ , K^+ , Ca^{2+} , and Mg^{2+} , which are used at 500 equivalent. The emission intensities are calculated from three independent experiments performed in duplicate.

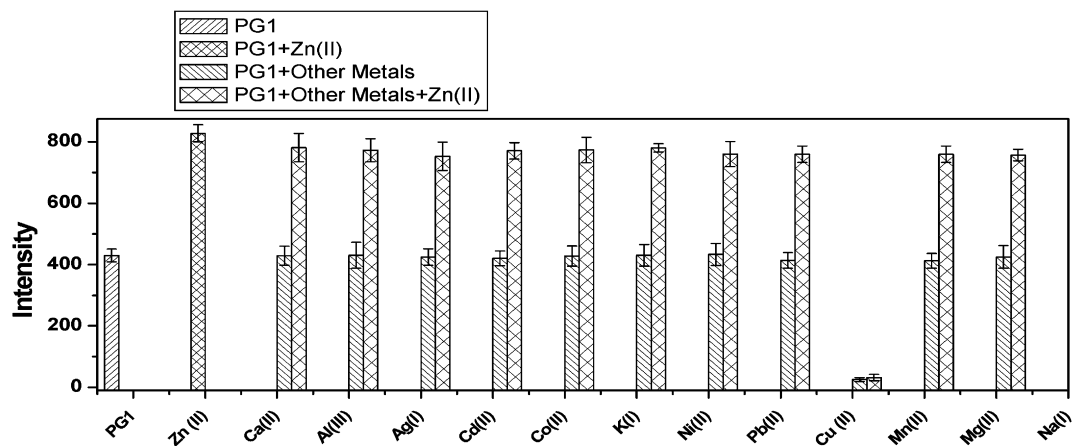


Figure 8. Emission intensity of **PG1** (10 μ M) in the presence of Zn^{2+} (1 equiv) and additional various metal ions at pH 7.4 (10 mM Hepes buffer). All metal ions are evaluated at one equivalent to Zn^{2+} except Na^+ , K^+ , Ca^{2+} , and Mg^{2+} , which are used at 500 equivalent. The emission intensities are calculated from three independent experiments performed in duplicate.

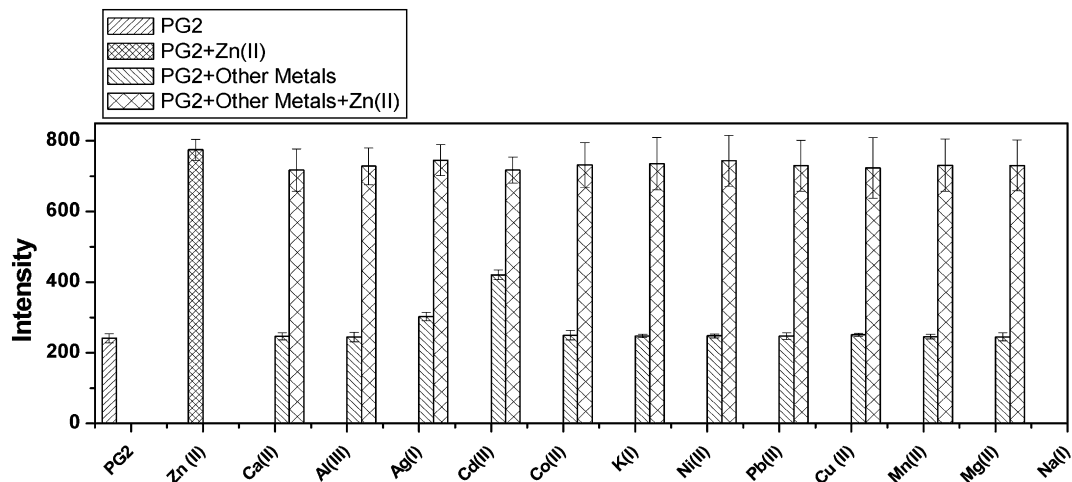


Figure 9. Emission intensity of **PG2** (10 μ M) in the presence of Zn^{2+} (1 equiv) and additional various metal ions at pH 7.4 (10 mM Hepes buffer). All metal ions are evaluated at one equivalent to Zn^{2+} except Na^+ , K^+ , Ca^{2+} , and Mg^{2+} , which are used at 500 equivalent. The emission intensities are calculated from three independent experiments performed in duplicate.

more potent-binding affinity for Zn^{2+} than did Cd^{2+} . It was concluded that **PG2** developed in this study had a great selectivity for Zn^{2+} .

2.6. Secondary structure of probe in the presence of metal ions

To investigate the secondary structure change of the peptide probes in the presence of metal ions, we measured the CD spectrum of the peptide probes in the presence of Zn^{2+} or Cu^{2+} . The CD spectra (Fig. 10) suggest that in the absence of metal ions, **GG2** may adopt a random coil and β sheet structures. However, the secondary structure of **GG2** changed in the presence of Cu^{2+} . **GG2** might adopt a random structure and a turn structure in the presence of Cu^{2+} on the basis of the weak negative band near 225 nm. The near-UV CD spectrum ranging from 250 to 300 nm, was measured because near-UV CD bands are used as an indication of the environment of aromatic residue such as Phe, Tyr, and Trp. Generally, near-UV CD bands are weaker than those in the far UV. ^{15b} The large positive band at 265 nm corresponding to the absorbance of dansyl group was observed in the CD spectrum measured in the presence of Cu^{2+} . The CD spectrum indicated that the environment of dansyl group was changed when **GG2**– Cu^{2+} was formed. The CD spectra and the large blue shift of the emission intensity in the presence of Cu^{2+} suggested that when **GG2** folded in the presence of Cu^{2+} , the hydrophilic environment around dansyl fluorophore could be changed into a hydrophobic environment.

The far UV CD spectrum of **PG1** in the presence of Zn^{2+} or Cu^{2+} indicated that **PG1** might adopt different secondary struc-

tures depending upon the presence of Zn^{2+} or Cu^{2+} . The far UV CD spectrum, including the negative band at 230 nm, indicated that **PG1** adopted more turn structures in the presence of Zn^{2+} than **PG1** did in the absence of metal ions, whereas **PG1** might adopt less turn structures in the presence of Cu^{2+} than **PG1** did in the absence of metal ions. The near-UV CD spectrum indicated that the environment of dansyl group was not greatly changed when **PG1** interacted with Zn^{2+} , whereas the environment of dansyl group was greatly changed when **PG1** interacted with Cu^{2+} . Far UV CD spectrum (200–230 nm) revealed that the secondary structure of **PG2** was not greatly changed when the peptide interacted with Zn^{2+} and **PG2** seemed to have a pre-organized structure for Zn^{2+} binding. However, a change of negative band at 240 nm indicated that the environment of dansyl was changed when the peptide– Zn^{2+} complex was formed. The CD spectrum indicated that **PG1** and **PG2** may adopt different turn structures in the absence of metal ions, and the secondary structure of the peptide probes plays an important role for detecting the specific metal ions. To validate the secondary structures of the peptide probes and to elucidate the metal-binding mode, we are currently investigating the secondary structure and folding of the peptide probes in the presence of metal ions by using NMR measurements.

Several research groups including that of the authors have synthesized various fluorescent probes for monitoring Zn^{2+} . ^{4b,13,19,20} because Zn^{2+} plays an important role in many biological and environmental processes. ^{1,2} The total concentration of Zn^{2+} in different cells varies from the nanomolar range up to about hundreds

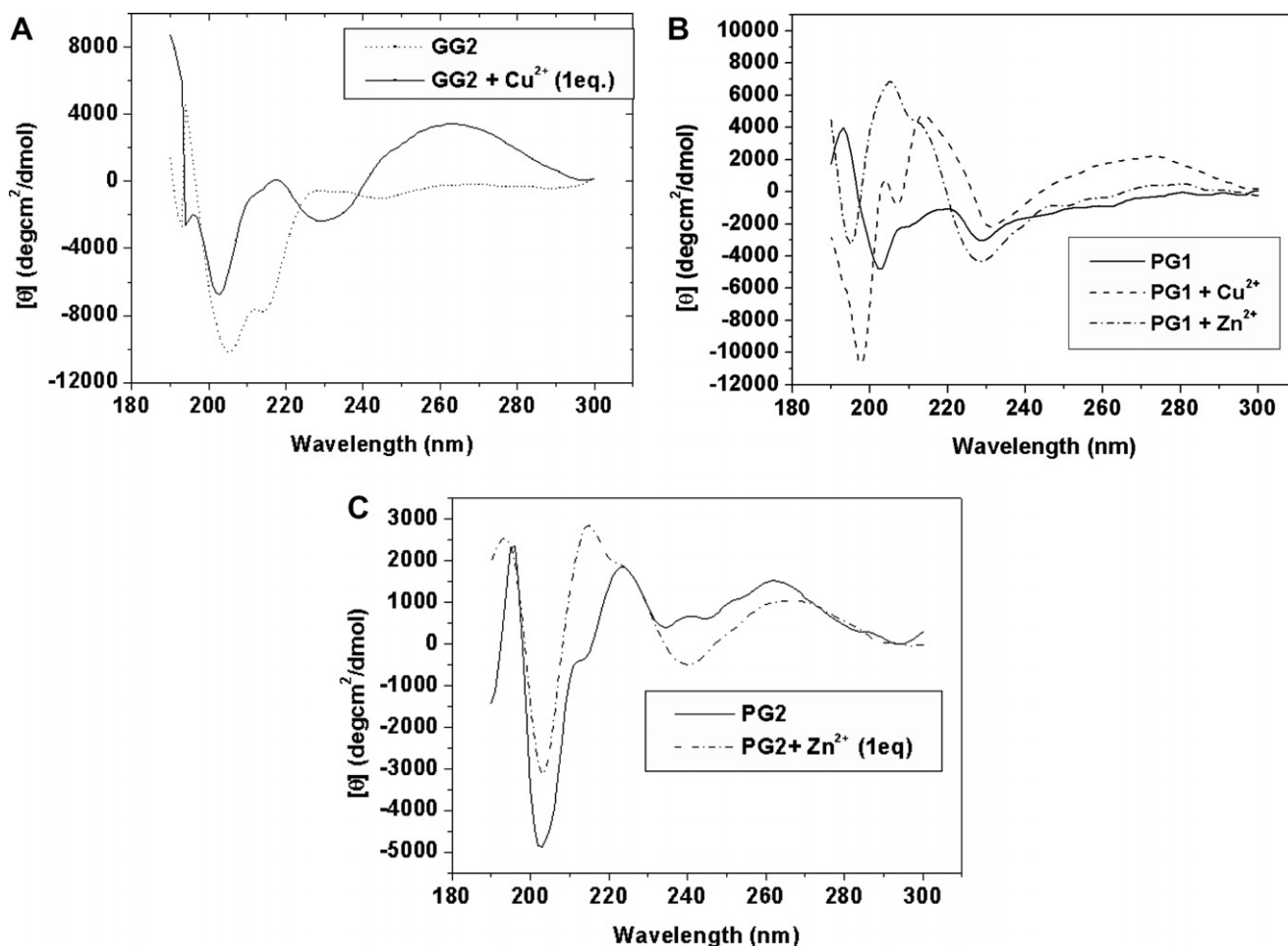


Figure 10. Near and Far UV CD spectrum of (A) **GG2**, (B) **PG1**, and (C) **PG2** in the presence of metal ions (1 equiv) in 10 mM Hepes buffer solution (pH 7.4).

micromolar.¹ Thus, optimized chemical probes are required to monitor zinc concentration ranging from nanomolar to micromolar. Even though several fluorescence-based chemical and peptide probes for Zn²⁺ have been reported, most of them suffered limitations due to tight-binding affinity (subnanomolar affinity) and interference of other metal ions. Specifically, the probes with micromolar-binding affinity for Zn²⁺ interacted with other transition metal ions.^{4b,13,19} Almost all chemical or peptide probes containing dansyl moiety and His (imidazole) residue were reported to show a large decrease of fluorescence emission intensity in the presence of Cu²⁺ due to the high affinity of the imidazole moiety for Cu²⁺ and the quenching effect of Cu²⁺.^{4b,8b,10b} Thus, the development of selective peptide probes with micromolar-binding affinity for Zn²⁺ remains a significant challenge. The peptide probe, **PG2**, developed in this study exhibited several advantages because of micromolar affinity for Zn²⁺ in physiological buffer solution, no interference of other metal ions, easy synthesis, and high solubility in a physiological buffer solution. Thus, we expect that the peptide probe has a great possibility to be used for monitoring extracellular and environmental Zn²⁺ concentration.

3. Conclusion

The overall study results confirmed the successful synthesis of selective fluorescent peptide probes for detecting Cu²⁺ or Zn²⁺, respectively, and demonstrated that the metal detecting selectivity was tuned by modulating the secondary structure. We also demonstrated that while a pre-organized secondary structure is not required for the selective detection of Cu²⁺ ion, it is required for the detection of Zn²⁺.

4. Experimental

4.1. General

Fmoc protected amino acids, *N,N*-diisopropylcarbodiimide, 1-hydroxybenzotriazole, and Rink Amide MBHA resin were purchased from Advanced ChemTech. Other reagents for peptide synthesis including trifluoroacetic acid (TFA), triisopropylsilane (TIS), dansyl chloride, triethylamine, diethyl ether, dimethyl sulfoxide (DMSO), *N,N*-dimethylformamide (DMF) and piperidine, were purchased from Aldrich.

4.2. Peptide synthesis

All peptide probes were synthesized using Fmoc-chemistry by solid-phase peptide synthesis, according to the literature procedure.¹⁴ The coupling of dansyl chloride was performed by applying the following procedure. To the resin bound peptide (65 mg, 0.05 mmol), dansyl chloride (40 mg, 0.15 mmol, 3 equiv) in DMF (3 ml) containing triethylamine (20 μ l, 0.15 mmol, 3 equiv) was added. Deprotection and cleavage were achieved by treatment with a mixture of trifluoroacetic acid (TFA)/TIS/H₂O (9.5:0.5:0.5, v/v/v) at room temperature for 3–4 h. After cleavage of the product from resin, the peptides were purified by preparative HPLC using a water (0.1% TFA)/acetonitrile (0.1% TFA) gradient (5–50% acetonitrile over 45 min). The peptide masses (**GG2** [M+H]⁺: calcd 848.48, obsd 848.60; **PG2** [M+H]⁺: calcd 928.26, obsd 928.79; **PG1** [M+H]⁺: calcd 888.24, obsd 888.47; **GG2-acm** [M+H]⁺: calcd 918.59, obsd 919.31; **PG2-acm** [M+H]⁺: calcd 998.37, obsd 999.34; **PG1-acm** [M+H]⁺: calcd 958.35, obsd 959.25) were characterized by ESI mass spectrometer (Platform II, Micromass, Manchester, UK) and MALDI TOF mass spectrometer (Voyager-DE STR, Applied Biosystem). The homogeneity (>95%) of the compound was confirmed by analytical HPLC on a C₁₈ column.

4.3. General fluorescence measurements

Fluorescence emission spectrum of a peptide probe in a 10 mm path length quartz cuvette was measured in 10 mM Hepes buffer solution (pH 7.4) using a Perkin-Elmer luminescence spectrophotometer LS 55 model. Sample concentration of peptide probe was confirmed by UV absorbance at 330 nm for dansyl group. Fluorescence spectra ranging from 350 to 650 nm were measured in the presence and absence of metal ions by excitation with 330 nm.

4.4. Determination of binding stoichiometry

The binding stoichiometry of peptides with metal ions was determined by using Job's plot.^{4a,21} A series of solutions with varying mole fraction of metal ions were prepared by maintaining the total peptide and metal ion concentration constant (e.g., [**GG2**]+[Cu²⁺] = 10 μ M, [**PG2**] + [Zn²⁺] = 2.5 μ M, [**PG1**] + [Cu²⁺] = 10 μ M and [**PG1**] + [Zn²⁺] = 5 μ M). The fluorescence emission was measured for each sample by exciting at 330 nm, and spectra were measured from 350 to 650 nm. The fitting data were acquired by plotting a straight line through the maximum or minimum emission intensity in the titration curve and were plotted against the mole fraction of the metal ion versus emission intensity.

4.5. Determination of association constants

The association constants were calculated based on the titration curve of the probes with metal ions. Association constants were determined by a nonlinear least squares fit of the data with the following equation:

$$F(x) = \frac{a + b * cx^n}{1 + cx^n},$$

where x is the concentration of metal ions, $F(x)$ is the intensity, a is the intensity of probe without metal ions, b is the intensity at the saturation, n is the binding stoichiometry, and c is the association constant.

4.6. Circular dichroism spectrum measurement

CD spectra were recorded on a Jasco J-715 spectropolarimeter (Tokyo, Japan) using a quartz cell of 1 mm path length between 190 and 300 nm at room temperature. The concentration of peptides was 150 μ g/ml in 10 mM Hepes buffer (pH 7.4). Two scans with a scan speed of 10 nm/min were averaged for each peptide. CD spectra were expressed as the mean residue ellipticity.

Acknowledgments

This work was supported by grants from Inha University. B. P. Joshi was recipient of a BK21 (II) fellowship.

References and notes

- (a) Lippard, S. J.; Berg, J. M. *Principles of Bioinorganic Chemistry*; Mill Valley, CA, 1994; (b) Muthaup, G.; Schlicksupp, A.; Hess, L.; Beher, D.; Ruppert, T.; Masters, C. L.; Beyreuther, K. *Science* **1996**, 271, 1406; (c) Valee, B. L.; Falchuk, K. H. *Physiol. Rev.* **1993**, 73, 79; (d) Berg, J. M.; Shi, Y. *Science* **1996**, 271, 1081; (e) Rossman, T. G. *Mutation Res.* **2003**, 533, 37.
- Merian, E. (Ed.), *Metals and their Compounds in the Environment*, VCH: Weinheim, 1991.
- (a) Kimura, E.; Koike, T. *Chem. Soc. Rev.* **1998**, 3, 179; (b) Rurack, K.; Resch-Genger, U. *Chem. Soc. Rev.* **2002**, 2, 116; (c) Kim, J. S.; Quang, D. T. *Chem. Rev.* **2007**, 107, 3780.
- (a) Hong, S. H.; Maret, W. *Proc. Natl. Acad. Sci. U.S.A.* **2003**, 100, 2255; (b) Shults, M. D.; Pearce, D. A.; Imperiali, B. *J. Am. Chem. Soc.* **2003**, 125, 10591; (c) Walkup, G. K.; Imperiali, B. *J. Am. Chem. Soc.* **1996**, 118, 3053; (d) Godwin, H. A.; Berg, J. M. *J. Am. Chem. Soc.* **1996**, 118, 6514.

5. (a) Torrado, A.; Walkup, G. K.; Imperiali, B. J. *Am. Chem. Soc.* **1998**, 120, 609; (b) Yujun, Z.; Jhony, O.; Andreopoulos, J. X.; Pham, M.; Fotios, S. M.; Leblanc, R. M. *J. Am. Chem. Soc.* **2003**, 125, 2680; (c) Brandt, M.; Madsen, J. C.; Bunkenborg, J.; Jensen, O. N.; Gammeltoft, S.; Jensen, K. J. *ChemBioChem* **2006**, 7, 623; (d) Serizawa, T.; Sawad, T.; Kitayama, T. *Angew. Chem., Int. Ed.* **2007**, 46, 723.
6. (a) Lakowicz, J. R. *Principles of Fluorescence*; Plenum Press: New York, 1983; (b) Rurack, K. *Spectrochim. Acta, Part A* **2001**, 57, 2161.
7. (a) Harris, K. L.; Lim, S.; Franklin, S. J. *Inorg. Chem.* **2006**, 45, 10002; (b) Petros, A. K.; Reddi, A. R.; Kennedy, M. L.; Hyslop, A. G.; Gibney, B. R. *Inorg. Chem.* **2006**, 45, 9941; (c) Reddi, A. R.; Guzman, T. R.; Breece, R. M.; Tierney, D. L.; Gibney, B. R. *J. Am. Chem. Soc.* **2007**, 129, 12815; (d) Bode, W.; Gomis-Ruth, R. X.; Stocker, W. *FEBS Lett.* **1993**, 331, 134; (e) Vallee, B. L.; Auld, D. S. *Biochemistry* **1990**, 29, 5647; (f) Hay, M. T.; Lu, J. H.; Richards, Y. *Proc. Natl. Acad. Sci. U.S.A.* **1996**, 93, 461; (g) Blindauer, C. A.; Sadler, P. J. *Acc. Chem. Res.* **2005**, 38, 62.
8. (a) Mal, T. K.; Ikura, M.; Kay, L. E. *J. Am. Chem. Soc.* **2002**, 124, 14002; (b) Zheng, Y.; Cao, X.; Orbulescu, J.; Konka, V.; Andreopoulos, F. M.; Pham, S. M.; Leblanc, R. M. *Anal. Chem.* **2003**, 75, 1706; (c) Zheng, Y.; Huo, Q.; Kele, P.; Andreopoulos, F. M.; Pham, S. M.; Leblanc, R. M. *Org. Lett.* **2001**, 3, 3277; (d) Parker, K. J.; Kumar, S.; Pearce, D. A.; Sutherland, A. J. *Tetrahedron Lett.* **2005**, 46, 7043; (e) Deo, S.; Godwin, H. A. *J. Am. Chem. Soc.* **2000**, 122, 174.
9. Cheng, R. P.; Fisher, S. L.; Imperiali, B. J. *Am. Chem. Soc.* **1996**, 118, 11349.
10. (a) Zhao, Y.; Zhong, Z. *Org. Lett.* **2006**, 8, 4715; (b) Koike, T.; Watanabe, T.; Aoki, S.; Kimura, E.; Shiro, M. *J. Am. Chem. Soc.* **1996**, 118, 12696.
11. (a) Eren, E.; Gonzalez-Guerreo, M.; Kaufman, B. M.; Arguello, J. M. *Biochemistry* **2007**, 46, 7754; (b) Banci, L.; Bertini, I.; Ciofi-Baffoni, S.; Finney, L. A.; Outten, C. E.; O'Halloran, T. V. *J. Mol. Biol.* **2002**, 323, 883; (c) Liu, J.; Stemmler, A. J.; Fatima, J. *Biochemistry* **2005**, 44, 51597.
12. Joshi, B. P.; Cho, W. M.; Kim, J.; Yoon, J.; Lee, K. H. *Bioorg. Med. Chem. Lett.* **2007**, 23, 6425.
13. (a) Fisk, J. D.; Gellman, S. H. *J. Am. Chem. Soc.* **2001**, 123, 343; (b) Haque, T. S.; Gellman, S. H. *J. Am. Chem. Soc.* **1997**, 119, 2303.
14. Fields, G. B.; Nobel, R. L. *Int. J. Pept. Protein Res.* **1990**, 35, 161.
15. (a) Chang, C. T.; Wu, C. S. C.; Yang, J. T. *Anal. Biochem.* **1978**, 91, 13; (b) Berova, N.; Nakanishi, K.; Woody, R. W. In *Circular Dichroism*; Wiley-VCH: New York, 2000. Chapter 21, pp 601–620.
16. (a) Raghothama, S. R.; Awasthi, S. K.; Balaram, P. J. *Chem. Soc., Perkin Trans. 2* **1998**, 137; (b) Andersen, N. H.; Olsen, K. A.; Fesinmeyer, R. M.; Tan, X.; Hudson, F. M.; Eidenschink, L. A.; Farazi, S. R. *J. Am. Chem. Soc.* **2006**, 128, 6101; (c) Kim, W.; McMillan, R. A.; Snyder, J. P.; Conticello, V. P. *J. Am. Chem. Soc.* **2005**, 127, 18121.
17. (a) Cabiaux, V.; Agerberth, B.; Johansson, J.; Homble, F.; Goormaghtigh, E.; Ruyschaert, J.-M. *Eur. J. Biochem.* **1994**, 224, 1019; (b) Sreerama, N. R.; Woody, W. *Biochemistry* **1994**, 33, 10022.
18. Association constants were obtained using the computer program ENZFITTER, available from Elsevier-BIOSOFT, 68 Hills Road, Cambridge CB2, 1LA, United Kingdom.
19. White, B. R.; Liljestr, H. M.; Holcombe, J. A. *Analyst* **2008**, 133, 65.
20. (a) Haugland, R. P. *Molecular Probes*, 6th; Eugene, OR, 1996; (b) Aoki, S.; Goto, H.; Kawatani, T.; Kimura, E.; Shiro, M. *J. Am. Chem. Soc.* **2001**, 123, 1123; (c) de Silva, A. P.; Gunaratne, H. Q. N.; Gunnlaugsson, T. A.; Huxley, T. M.; McCoy, C. P.; Rademacher, J. T.; Rice, T. E. *Chem. Rev.* **1997**, 97, 1515; (d) Ajayaghosh, A.; Carol, P.; Sreejith, S. J. *Am. Chem. Soc.* **2004**, 127, 14962. and reference therein; (e) Nolan, E. M.; Jaworski, J.; Okamoto, K.; Hayashi, Y.; Sheng, M.; Lippard, S. J. *J. Am. Chem. Soc.* **2005**, 127, 16812.
21. (a) Beck, M. T.; Nagypal, L. *Chemistry of Complex Equilibria*; Halsted Press: New York, 1990. pp 112–118; (b) McBryde, W. A. E. *Talanta* **1974**, 21, 979; (c) Likussar, W. D.; Boltz, F. *Anal. Chem.* **1971**, 43, 1265; (d) Vosburgh, W. C.; Cooper, G. R. *J. Am. Chem. Soc.* **1941**, 63, 437.